Multimodal general expectancy effects elicited without influencing sensory representations

Ziyue Hu[1], Dominic M. D. Tran[1], & Reuben Rideaux[1,2*]

[1]School of Psychology, The University of Sydney, Camperdown, Australia
[2]Queensland Brain Institute, The University of Queensland, St Lucia, Australia
*corresponding author: reuben.rideaux@sydney.edu.au

Conflict of interest statement: The authors declare no competing interests.

Acknowledgements: This work was supported by an Australian Research Council Discovery Early Career Researcher Award and (DE210100790) a National Health and Medical Research Council Investigator Grant (2026318) to RR, as well as an Australian Research Council Discovery Early Career Researcher Award (DE220100829) to DT.

Keywords: vision, predictive coding, temporal expectation, EEG, pupillometry.

Author contributions: ZH collected the data and wrote the initial version of the manuscript. RR analysed the data and supervised the study. All authors contributed to experimental design, data interpretation, and revising the manuscript.

ABSTRACT

Predictive coding theories posit a reduction in error-signalling neural activity when incoming sensory input matches existing expectations – a phenomenon termed *expectation suppression*. While human neuroimaging studies have consistently reported reduced neural activity for expected events, it is uncertain whether this reduction arises from the *sharpening* or *dampening* of neurons selective for expected features. A further aspect of predictive coding that remains untested is how predictions are integrated across sensorimotor domains. To investigate these two questions, we employed a novel cross-domain probabilistic cueing paradigm, where participants were presented with both visual and motor cues within a single trial. These cues manipulated the orientation and temporal expectancy of target stimuli with 75% validity. Participants completed a reproduction task where they rotated a bar to match the orientation of the target stimulus while their neural and pupil responses were respectively measured via electroencephalography and eye tracking. Our results showed an effect of expectancy in the motor condition across multiple measures, while evidence in the visual condition was inconsistent. However, no differences in orientation fidelity were found in sensory representations between expected and violation trials for either domain. These findings show that violations of temporal expectancy produce prediction error signals that do not influence sensory representations. Further, the findings add to a growing body of work casting doubt on the effectiveness of probabilistic cueing paradigms for eliciting prediction errors. Due to null findings in the visual and representational analyses, we did not further investigate cross-domain prediction integration.

1. INTRODUCTION

Predictive coding frameworks challenge traditional views of perception as a bottom-up process, driven solely by the sensory reality (Kuffler, 1953). Instead, these frameworks propose that perception emerges through a dynamic interplay between incoming sensory inputs and pre-existing expectations (Friston, 2005, 2010; Lotter et al., 2020; Rao & Ballard, 1999). For example, our interpretation of an object's convexity may depend on implicit assumptions regarding the typical direction of light sources (Sun & Perona, 1998). Within this framework, the brain is thought to continuously compare feedforward sensory input with internal generative models, whereby prediction errors – mismatches between input and expectations – propagate back through cortical hierarchies to update and refine these models (Friston, 2005). This iterative process is thought to optimize metabolic efficiency by minimizing the energy expenditure required for representing and engaging with the environment (Friston, 2005, 2010).

1.1. Expectation Suppression and Underlying Neural Mechanism

Predictive processing is substantiated by a growing body of evidence (de Lange et al., 2018; Kok et al., 2012, 2017; Rideaux et al., 2024; Summerfield et al., 2011; Tang et al., 2018; Tran & Livesey, 2021). For instance, studies using functional magnetic resonance imaging (fMRI) and magnetoencephalography (MEG) show that auditory cues linked to specific visual stimuli can elicit anticipatory neural activity resembling perception, even in the absence of external stimuli (Kok et al., 2014, 2017). These findings highlight the brain's active role in generating internal models to predict and interpret sensory information. The ability to form and leverage such expectations is thought to streamline processing demands (Friston, 2005, 2010), often evidenced by reduced neural activity in response to expected stimuli – a phenomenon known as *expectation suppression* (Kok et al., 2012; Summerfield et al., 2008; Tang et al., 2018). For example, recent transcranial magnetic stimulation (TMS) work in the motor domain reported reduced motor evoked potential (MEP) amplitude for predictable self-actions (Tran et al., 2021) relative to unexpected stimulation. Similar reduction in neural activity for expected events has been observed across other sensory modalities and neuroimaging techniques, including electroencephalography (EEG) measured event-related potentials (ERP) in auditory (N1, Harrison et al., 2021) and

visual modalities (P300, Saurels et al., 2022; N1 and P1, Tang et al., 2018). These findings suggest that expectation suppression applies across different sensory modalities, reflecting a domain-general mechanism by which the brain optimizes processing efficiency when dealing with expected stimuli. However, the neural mechanism underlying this phenomenon remain contested.

One popular interpretation from the predictive coding framework is that the observed expectation suppression arises from the *sharpening* of neurons tuned to expected events, resulting in more precise neural representations compared to unexpected events (Kok et al., 2012; Kok & de Lange, 2015). Supporting this view, Kok et al. (2012) employed multivariate pattern analysis (MVPA) on fMRI blood-oxygen-level-dependent (BOLD) signals and found higher classification accuracy for expected (compared to unexpected) stimuli, suggesting that expected events are represented more precisely in the brain. This findings aligns with other neuroimaging evidence supporting the sharpening account (Den Ouden et al., 2008; Todorovic et al., 2011). Psychophysical evidence further corroborates this account; Kok et al. (2012) found that participants could more accurately detect differences in orientation and contrast when stimuli were expected. Similarly, Teufel et al., (2018) reported lower detection and discrimination thresholds for expected stimuli. These findings suggest that expected events are represented with better fidelity, consistent with the sharpening account of predictive coding.

Although the sharpening account has gained some empirical support, an alternative hypothesis has been proposed in recent years; that is, expectation suppression may instead arise from the inhibition of neurons selective for expected features, leading to the reduction of representational fidelity for expected events (de Lange et al., 2018; Tang et al., 2018, 2023). This *dampening* of neurons tuned to the expected feature would instead result in unexpected events being represented relatively more precisely than expected events. Tang et al. (2018) investigated this account using inverted encoding modelling – a technique that predicts neural responses to specific stimulus features by mapping how these features are represented across continuous dimensions in the brain (Brouwer & Heeger, 2011; Harrison et al., 2023; Rideaux, 2024). Unlike MVPA, which simply attempts to discriminate between multiple neural patterns (Gessell et al., 2021; Kok et al., 2012),

inverted encoding produces continuous feature-specific predictions, enabling finer analyses of sensory encoding. Using this approach, Tang et al. (2018) found higher representational fidelity for unexpected orientations compared to those that were expected, supporting the dampening account. Similar results have been observed across other studies on low-level features (Smout et al., 2019) and non-human animals (awake and anaesthetized mice, Tang et al., 2023). Therefore, contrary to the sharpening account of predictive coding (Friston, 2005; Kok & de Lange, 2015), recent neuroimaging findings suggest that unexpected events may instead have better representational fidelity in the brain. Consistent with this hypothesis, Rideaux et al., (2024) used a task where participants replicated stimulus orientations by rotating a bar – allowing errors in these continuous responses to directly index representational fidelity – and found faster and more precise responses for unexpected stimuli. Similar behavioural evidence, corroborated by electrophysiological recordings, supporting the dampening account were found in another recent study investigating the influence of temporal context of visual processing (Lee & Rideaux, 2024). Thus, evidence from behavioural work seems to exhibit a similar inconsistency as that from neuroimaging experiments.

1.2. Cross-domain Prediction

Addressing whether expectation suppression arises from sharpening or dampening of neurons selective to expected events remains a challenging endeavor. Beyond these competing accounts, a yet unexplored question that may provide insight into the representational fidelity debate concerns how predictions from different sensory modalities (e.g., vision and audition) or domains (e.g., vision and motor) interact. Traditional multimodal perception studies typically present participants with stimulus information from two different sensory modalities, and task them with responding to some aspect of the stimuli that is influenced by their integration. For example, Alais and Burr (2004) presented participants with both visual and auditory stimuli, manipulating the reliability of each to investigate how the brain integrates bimodal sensory information to infer the spatial location of a single event. While this form of multimodal experimental design has been used extensively to study how the brain integrates low-level features (Alais & Burr, 2004; Buhmann et al., 2024; Rideaux et al., 2021; Rideaux & Welchman, 2018; Stanford et al., 2005; Stein &

Stanford, 2008), it has not yet been implemented within the context of predictive processing, namely, to study how the brain integrates higher-level sensory expectations. Several predictive coding studies have employed multiple sensory modalities or domains, but so far this has been applied in the context of considering predictions formed in one modality or domain which signals the event probability in another (Kok et al., 2012, 2014, 2017; Stekelenburg & Vroomen, 2015). For instance, Kok et al. (2012) used auditory cues to predict the orientation (45° or 135°) of visual target stimuli. Another study by Tran et al. (2025) simultaneously measured motor predictions using MEPs and auditory predictions using ERPs. They found that the strength of error signaling in one domain predicted the strength of error signaling in the other. The results suggest that predictions across different domains are related, and they support the notion that predictive coding may be governed by domain general mechanisms. However, this study did not investigate the fidelity of the neural representations or how predictions across domains were integrated. Thus, it remains unclear how predictions from different domains integrate to represent a single event. In natural settings, the integration of predictive signals from multiple sensory modalities or domains is essential for a wide range of activities, from simple daily tasks (e.g., catching a falling object) to complex athletic performances (e.g., predicting the trajectory of a ball and timing a precise hit). These examples highlight the importance of adopting a cross-domain perspective on predictive processing.

1.3. Current Study

To address the sharpening versus dampening debate and the gap in our understanding of cross domain predictions, this study employed a novel cross domain probabilistic cuing paradigm. We presented participants with both visual and motor cues, which respectively manipulated the featural (orientation) and temporal expectancy of the target stimuli with 75% validity. To assess the representational fidelity of (un)expected events, we combined inverted encoding modelling of EEG data with a continuous reproduction task to assess both neural and behavioural evidence, respectively. We hypothesized that participants' neural decoding and behavioural responses would either be more precise for expected events, aligning with the sharpening account, or for unexpected events, based on the dampening account. In addition, we used a counterbalanced 2x2 (visual/motor,

expected/violation) design to examine whether such expectancy effects from multiple domains combine additively, as observed for other forms of cue integration (Stanford et al., 2005).

Consistent with previous studies (e.g., Hall et al., 2018; Kok et al., 2012; Tang et al., 2018), we did not explicitly disclose the cue-target association to the participants. However, to cross-validate whether we had successfully manipulated expectation, we also recorded participants' pupil diameter, as pupil dilation is a physiological index of surprise (Lavín et al., 2013), and has been adopted in previous studies (Mazancieux et al., 2023; Rideaux et al., 2024). By simultaneously recording neural, behavioural, and physiological responses to expectation, we sought to provide a comprehensive view of how expectancy shapes sensory processing.

2. METHODS

2.1. Participants

58 first- and second-year psychology students were recruited from the University of Sydney, with five participants excluded for misunderstanding of the task and two for major technical corruptions of the EEG data. The final sample size (n = 51, $\mathrm{M}_{age} = 20.23, \mathrm{N}_{male} = 7$) was similar to previous experiments using similar neural decoding methods (Harrison et al., 2023; Rideaux, 2024; Rideaux et al., 2023). Since the experiment was largely visual, participants were required to have normal or corrected-to-normal vision (assessed using a standard Snellen eye chart). Participants were all naïve to the aims of the study, and the experiment protocol was approved by the University of Sydney's Psychology Low Risk Human Ethics Committee.

2.2. Apparatus

The current study was conducted in a dark, sound-proof, and electromagnetically shielded room. Task stimuli were displayed on a mid-grey disc centred on a black background, to reduce orientation cues provided by the edges of the screen. Stimuli were presented on a display monitor (ASUS VG248QE 144 Hz 24'' 1920x1080 HDMI Gaming Monitor) via MATLAB R2020a (The MathWorks, Inc., Matick, MA) and PsychToolbox (v3.0, http://psychtoolbox.org/; Pelli, 1997). Participants were instructed to place their head on a chin-forehead rest, controlling the viewing distance at 70 cm with the screen subtended to 41.47° x 23.33°.

2.3. Stimulus

Referring to **Figure 1**, the target stimulus consisted of two wedges arranged apex-to-apex, creating a bowtie configuration (orientation randomly sampled from between 0 and 180°), which focused participants' attention on the screen centre. To establish visual expectations in participants, a visual cue was introduced before the target stimuli, consisting of two aligned white lines displayed outside the region of the target stimuli. This design was intended to prevent adaptation in the region of the visual field where the target was presented (Rideaux et al., 2023) and maintain participants' focus on the centre of the screen. To encourage participants' use of the visual cue, the visibility of the target stimulus was reduced by presenting it briefly (100

ms) at low contrast (0.1 relative to maximum screen contrast). Additionally, a motor cue – a green dot placed at the centre of the screen – was presented to prompt participants to press the left mouse button.

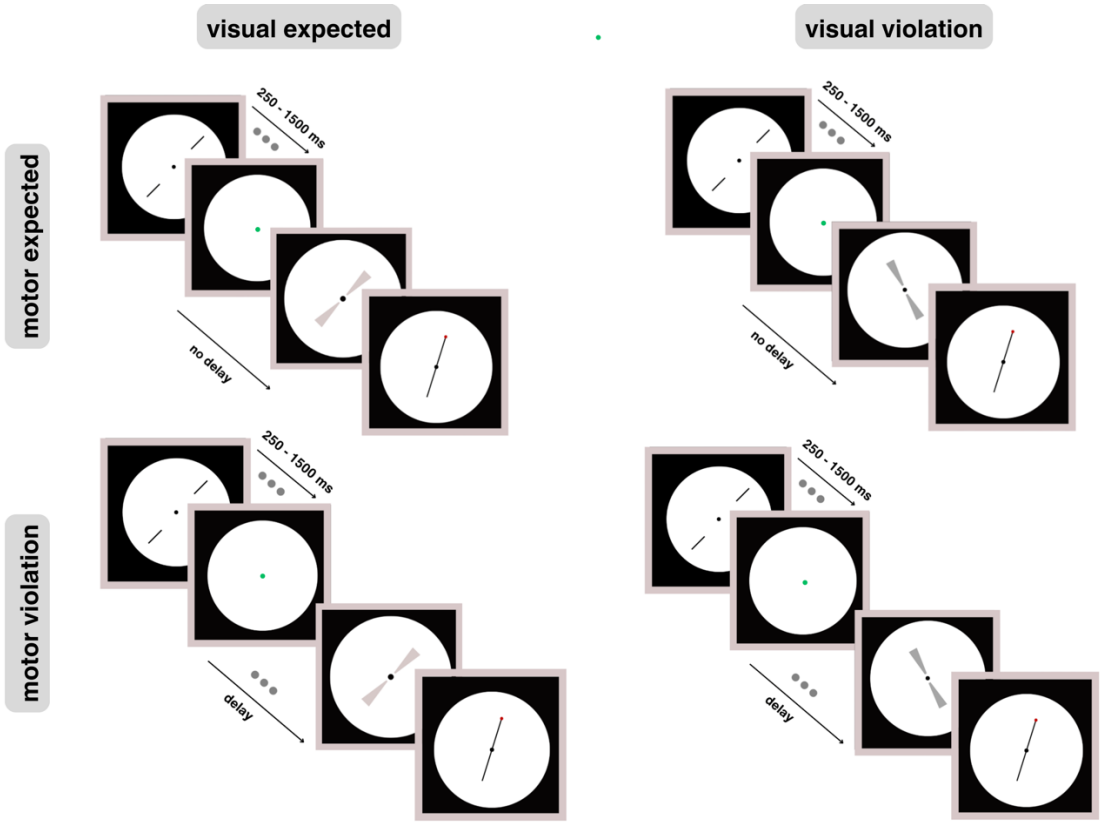

Figure 1. Experimental manipulation of visual and motor expectation. Each trial began with a visual cue, followed by a variable delay (250-1500 ms) before a motor cue prompted participants to press the left mouse button. The target stimulus appeared either immediately (*motor expected; top row*) or after an additional variable delay (*motor violation; bottom row*), with its orientation either matching (*visual expected; left column*) or differing from the visual cue (>30°; *visual violation; right column*). Participants reported the target's orientation by rotating a black line, with a red dot indicating the response index. Note, the depiction provided above does not accurately represent the actual stimuli viewed by participants and is for illustrative purpose. The grey circle on the background has been changed to white, whilst the colour of the visual cue has been illustrated as a pair of aligned black lines.

2.4. Design

Each trial began with the presentation of a visual cue for 500 ms, followed by a variable delay (250–1500 ms). Participants were then prompted by a motor cue to press the left mouse button. Upon release of the button, the target stimulus either appeared immediately (*motor expected*) or after a variable delay (*motor violation*), which was uniformly sampled from one-third of the motor-visual cue delay range. The orientation of the visual cue either matched the target (*visual expected*) or differed significantly (>30°; *visual violation*). Participants reproduced the target's orientation

using a mouse-controlled black line, with the initial angular position randomized to prevent response bias. To facilitate responses, a red dot indicated the reproduction index during the response phase.

There were 2 (visual expectancy: expected/violation) x 2 (motor expectancy: expected/violation) conditions in the current study (see **Figure 1**). Trials from each condition were pseudo-randomly interleaved within each block. There were 10 blocks in total, with 72 trials for each block. Visual expectancy trials comprised 75% expected trials and 25% violation trials. Similarly, motor expectancy trials contained 75% expected trials and 25% violation trials. The two conditions were counterbalanced. For example, 75% of visual expected trials were also motor expected trials (see **Figure 2**). This design allowed us to explore how sensory representations change dynamically when predictions from both visual and motor domains are met, only one of them is met, or both are violated.

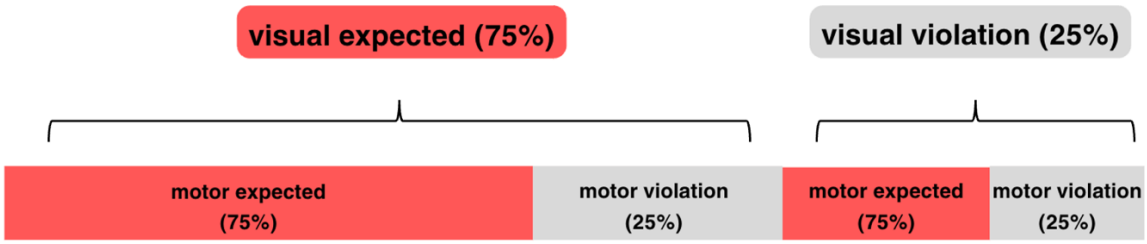

Figure 2. Example of counterbalancing four conditions (visual/motor expectancy). In each block, 75% of trials fell under the visual expected condition, with these further divided into 75% motor expected and 25% motor violation trials. The remaining 25% of trials were visual violation trials, maintaining the same 3:1 distribution of motor expected and violation trials. Consequently, the visual expected/motor expected trials constituted 56.25% of the total trials, while both the visual expected/motor violation and visual violation/motor expected trials each made up 18.75%. The double-violation condition, involving both visual and motor violations, comprised 6.25% of the total trials.

There were two potential confounds that could have contributed to differences between expected and violation conditions. First, there were more three times more expected trials than violation trials, which could lead to higher EEG decoding accuracy in the expected condition. Second, the additional temporal delay between the visual cue and target in the motor violation condition may have, for example, disadvantaged behavioural reproduction of the target violation trials. These potential confounds were anticipated during the design of the experiment and to mitigate them, we used a variable visual-to-motor-cue delay (250 - 1500 ms), so that by omitting 66% of trials from the expected condition with longer visual-to-motor-cue delays from the

analysis we could simultaneously match the number and duration of trials between conditions.

2.5. Procedure

Before the experiment, participants were provided with written and verbal instructions. They were informed that each trial would initiate with two aligned white lines, followed by the appearance of a green dot, prompting them to press the left mouse button. After their button-pressing response, the target pattern would appear, and the participant would be required to reproduce its orientation. Nevertheless, the relationships between visual/motor cue with the target stimulus were not explicitly disclosed. Participants completed a brief practice session with feedback (a red line indicating the correct orientation), but no feedback was provided during the testing session.

2.6. EEG Recording and Pre-processing

This study employed 64-channel active Ag/AgCl electrodes with the arrangement on the scalp aligning with the 10–20 international standard (Oostenveld & Praamstra, 2001), via a nylon cap and an online reference point at FCz. EEG data were captured at a 1024 Hz sampling rate using a 24-bit A/D conversion and recorded on a BrainVision ActiCap system (Brain Products GmbH, Gilching, Germany). The EEG data pre-processing was conducted using EEGLAB version 2021.1 (Delorme & Makeig, 2004). The data sampling rate was initially reduced to 256 Hz. To eliminate slow baseline fluctuations, a 0.1 Hz high-pass filter was applied, and a 45.0 Hz low-pass filter was employed to filter out high-frequency noise and artifacts. The final data were epoched from -200 ms to 500 ms relative to the onset of the target stimulus, and for *post hoc* analyses, the motor cue.

2.7. Eye Tracking

Participants' pupil responses were recorded via an Eyelink 1000 high-speed camera (version 4.594, SR Research Ltd., Mississauga, Ontario, Canada) that interfaced with an eye-tracking control monitor (Eyelink host PC). Participants' pupillary responses during the experiment were monitored by the experimenter via a 1 kHz live video feed of the right eye displayed on the control monitor.

2.8. Data Analysis

2.8.1. Behavioural Response and Mixture Modelling

In the behavioural reproduction task, we recorded both response time and replication performance (i.e., the angular difference between participants' responses and the target orientation), with a focus on replication performance as the dependent variable of interest in the analysis. A preliminary analysis of circular standard deviation of replication performance (referred to as '*response error*') revealed large standard errors in the current dataset. Therefore, to better understand the nature of errors, we utilized a mixture modelling approach similar to previous working memory literature (Zhang & Luck, 2008), to disambiguate trials on which participants were replicating the target orientation or merely guessing. Guess responses exhibit a uniform distribution of errors, showing no relationship with the target orientation. Conversely, valid replication of the target orientation would manifest as a distribution of errors centered on the target. The width of this distribution is inverse to participants' behavioural precision, referred to as κ. A mixture model comprising a combination of these two distributions was fit to each participant's data.

2.8.2. Univariate Analysis of EEG data

Target stimuli in the current study were orientation-based, with orientation-selective neuron activities typically observed over occipital channels (Roe et al., 2012). Therefore, we defined an occipital region of interest (ROI) including all occipital and parietal electrodes.

2.8.3. Inverted encoding Modelling

To identify the neural representations of the target stimuli, we utilized an inverted modelling approach to decode the target stimuli's orientation from EEG recordings, consistent with previous work (Brouwer & Heeger, 2011; Harrison et al., 2023; Rideaux, 2024; Tang et al., 2018). We first developed a forward model that described the EEG activity in response to the target stimuli's orientation. This model then served as a basis to build an inverse model that could interpret the EEG data to ascertain the orientation of the target stimuli. In the analysis, we applied a ten-fold cross-validation approach, wherein we trained the inverse model with 90% of the data set and then tested its accuracy by decoding the orientation from the remaining 10% of the data.

Consistent with the previous literature (Harrison et al., 2023; Rideaux, 2024), the forward model consisted of five hypothetical channels with linearly spaced orientation preference between 0° and 180°. Each channel was expressed as a half-wave sinusoid raised to the fourth power. Therefore, the turning curve for each specific orientation would be described as a weighted sum of the five channels. The EEG activity observed for each presentation can be characterised using the following linear model:

$$\mathbf{B} = \mathbf{WC} + \mathbf{E} \tag{1}$$

where **B** (*m* sensors x *n* representations) denotes the EEG data, **W** is a weight matrix (*m* sensors x 5 channels) to be estimated, **C** (5 channels x *n* representations) represents the nominated channel activities, **E** stands for residual errors.

To train an accurate inverse model, we sought to compute the weights that would reconstruct channel activities in EEG data with minimal error. Adapting from previous M/EEG work (Kok et al., 2017; Mostert et al., 2015), due to high correlations between signals recorded at adjacent sensors, we modified the conventional inverted encoding model approach to include noise covariance to enhance EEG data modelling accuracy. We also normalized components **B** and **C** to zero mean across presentations for each sensor and channel. The model was refined through a subset of data selected via the ten-fold cross-validation. Hypothetical responses for each of the five channels were derived from the training data, forming a response vector $\boldsymbol{c}_{train,i}$ for each channel $\boldsymbol{i}$, in proportion to the number of training presentations (n_{train}). Sensor weights $\boldsymbol{w_i}$ were then calculated using least squares estimation as following:

$$\boldsymbol{w_i} = (\boldsymbol{c}_{train,i}\boldsymbol{c}_{train,i}^{\mathbf{T}})^{-\mathbf{1}}\boldsymbol{c}_{train,i}^{\mathbf{T}}\boldsymbol{B}_{train} \tag{2}$$

such that, $\boldsymbol{B}_{train}$ (*m* sensors x *n* representations) denotes the EEG data training the forward model. Following this, we calculated the optimal spatial filter $\mathbf{v}_{\boldsymbol{i}}$ to reconstruct *i*th channel activity (Mostert et al., 2015) using:

$$\boldsymbol{v_i} = \frac{\tilde{\Sigma}_i^{-1}\boldsymbol{w_i}}{\boldsymbol{w}_i^{\mathrm{T}}\tilde{\Sigma}_i^{-1}\boldsymbol{w_i}} \tag{3}$$

where $\tilde{\Sigma}_i$ represents the regularized covariance matrix for channel *i*. Since adding noise covariance to the filter estimation could effectively reduce noise caused by high neighbouring sensor correlations, we estimated noise covariance in the following step. To enhance noise suppression, we further refined our estimation through

regularization by shrinkage, which employed an analytically determined optimal shrinkage parameter (Mostert et al., 2015), forming a regularized covariance matrix $\tilde{\Sigma}_i$ via:

$$\hat{\Sigma}_i = \frac{1}{n_{\text{train}}-1} \boldsymbol{\varepsilon_i} \boldsymbol{\varepsilon_i}^{\mathrm{T}} \tag{4}$$

$$\boldsymbol{\varepsilon_i} = \mathbf{B}_{train} - \boldsymbol{w_i} \boldsymbol{c}_{train,i} \tag{5}$$

where n_{train} stands for the number of training representations. Adding up the spatial filters $\mathbf{v_i}$ for all five orientation channels formed a channel filter matrix V (*m* sensors x 5 channels), which could then be used to reconstruct channel responses in testing set via:

$$\mathbf{C}_{test} = \mathrm{V}^{\mathrm{T}} \mathbf{B}_{test} \tag{6}$$

Subsequently, we decoded the orientation for each presentation by transforming the reconstructed channel responses to polar form as following:

$$z = \mathbf{c} \cdot e^{2i\varphi} \tag{7}$$

and then computing the estimated angle using:

$$\hat{\theta} = \frac{\arg(z)}{2} \tag{8}$$

where $\mathbf{c}$ represents a vector of channel responses and $\boldsymbol{\varphi}$ is the vector of preferred angles for the channels, which was multiplied by two to map the 180° orientation space onto a 360° space. Based on the orientations decoded by our proposed model, we estimated the model's decoding *accuracy*, defined as the similarity between the decoded orientation and actual presented orientation (Kok et al., 2017). It was characterized by projecting the decoded-presented orientation differences onto a vector oriented at $0°$:

$$\hat{r}_\theta = \mathrm{Re}\,[\bar{R}],\ \ \bar{R} = \frac{1}{n}\sum_{j=1}^{n} \exp\left(\mathrm{i}(\hat{\theta}_j - \theta)\right) \tag{9}$$

2.8.4. Linear Discriminant Analysis

Linear discriminant analysis (LDA) is a dimensionality reduction technique used in classification to find a linear combination of features that optimally separates different classes (Subasi, 2020). After finding null effects in the inverted encoding modelling, we further performed a *post hoc* analysis, where we applied LDA to the EEG data to test whether the trials from the current dataset (visual and motor conditions) could be classified based on trial expectancy (expected/violation).

Classification accuracy indices were generated separately for visual and motor conditions.

2.8.5. Pupillometry data

Pupillometry recordings were epoched to a duration of -500 to 1500 ms around the target stimulus presentation. Data were pre-processed by removing blinks (100 ms buffer window), removing outliers (median absolute deviation>2.5), interpolated, bandpass filtered with a first-order Butterworth filter (highpass=15.6 Hz, lowpass=500 Hz), *z*-scored, epoched, and down-sampled to 125 Hz, respectively. These epochs were then accordingly grouped into four experimental conditions (visual and motor expected/violation).

2.9. Statistical Analysis

2.9.1. Behavioural Analysis

Repeated-measure ANOVAs (2x2: visual/motor, expected/violation) were conducted on response error, reproduction precision, and guess rate. Bayes Factors (BF; Jeffreys, 1998) were calculated to compare statistical support for both null and alternative hypotheses.

2.9.2. Cluster Correction and Bayesian t-test of Time-Series Data

EEG and pupillometry yield time-series data. Using multiple paired *t*-tests to analyse time-series data at each time point can lead to a high risk of Type I error, so cluster-based permutation tests were employed to address multiple comparisons (Maris & Oostenveld, 2007). The analysis included 358 (time points) comparisons per test with 10,000 permutation samples, and a cluster-forming alpha of .05 (Bode et al., 2019). For each permutation sample, expectancy condition (expected/violation) labels were shuffled and paired *t*-tests were conducted at each time point. Clusters were formed from *t*-values with *p*-values <.05, with adjacent time points treated as temporal neighbours. The sum of *t*-values within a cluster was defined as the cluster's 'mass'. The largest cluster masses from the 10,000 permutation samples formed the null distribution, against which the cluster masses from the original dataset were compared. The cluster-corrected significance of each cluster was determined by its percentile rank relative to the null distribution. This approach thus effectively controls the family-wise error rate while remaining sensitive to detecting effects in temporally

autocorrelated EEG and pupillometry data (Groppe et al., 2011; Maris & Oostenveld, 2007). To test the effect of expectancy on univariate and multivariate EEG data (inverted encoding modelling and LDA) and pupillometry responses, we conducted permutation paired *t*-tests to compare visual/motor expected and violation trials, and significant time periods were interpreted as those of mass exceeding the 95th percentile of the null distribution. The Bayes factor for each time point was also calculated to evaluate evidence for both null and alternative hypotheses. Although the study initially aimed to examine additive effects of cross-domain predictions, the null results in most visual condition analyses precluded cross-domain analysis.

2.10. Data and code availability

The data and code for this study will be made available upon reasonable request.

3. RESULTS

3.1. Effect of Expectancy and Sensorimotor Domain on Response Error

To investigate how expectancy modulates perceptual fidelity, we first analyzed the effects of sensorimotor domain (visual vs. motor) and expectancy (expected vs. violation) on response error (σ°), which was measured as the circular standard deviation of the angular differences between the target orientation and participants' response. As shown in **Figure 3**, A 2×2 repeated-measures ANOVA revealed a significant main effect of expectancy ($F_{1,51}$=27.393, P<.001, BF_{10}=9917.040), with larger errors in violation trials, but no significant main effect of sensorimotor domain ($F_{1,51}$=0.016, P=.899, BF_{10}=0.139). The interaction effect was also not significant ($F_{1,51}$=1.683, P=.200, BF_{10}=0.322), with Bayesian analysis providing anecdotal evidence favouring the null hypothesis.

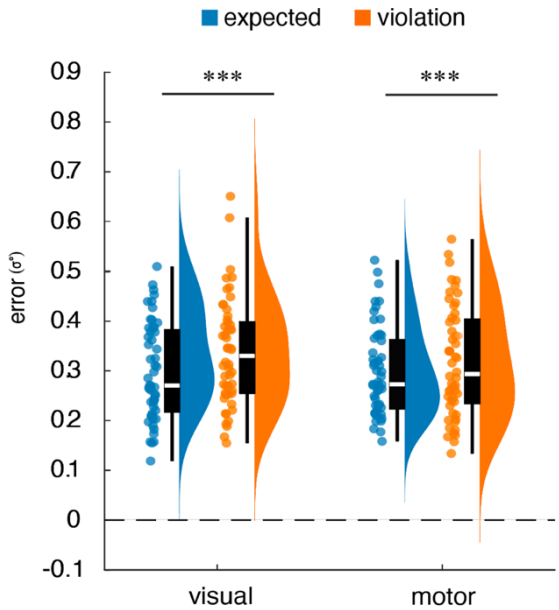

Figure 3. Response error by sensorimotor domain and expectancy. Violin plots visualize the distribution of response errors for each condition, with the median indicated by boxplots within each violin and dots indicate individual participant data points. Significant results ($p < .001$) are marked with ***.

3.2. Response Error: Replication Precision and Guess Rate Analysis

To further investigate the source of the increased errors in violation trials, mixture modeling was used to differentiate participants' behavioral responses based on replication precision and guessing (Bays & Husain, 2008; Zhang & Luck, 2008). **Figure 4A** illustrates the effects of sensorimotor domain and expectancy on replication precision (κ), where higher κ values indicate more precision. A 2×2

435 repeated-measures ANOVA revealed no significant main effect of domain
436 (($F_{1,47}$=0.306 P=.582) or expectancy ($F_{1,47}$ =0.162, P=.581), both with substantial
437 evidence for the null hypothesis indicated by the Bayes factor (BF_{10}=0.162). There
438 was also no significant interaction effect between domain and expectancy
439 ($F_{1,47}$=3.194, P=.080) with the Bayes factor providing anecdotal evidence for the null
440 hypothesis (BF_{10}=0.673). Similarly, for guess rate (frequency of guessing; **Figure 4B**),
441 there was no significant main effect of domain ($F_{1,46}$ =0.125, P=.724, BF_{10}=0.147), but
442 there was a significant main effect of expectancy, with higher guess rates in violation
443 trials than expected trials ($F_{1,46}$ =26.342, P<.001, BF_{10}=6982.405). The interaction
444 effect was not significant ($F_{1,46}$ =2.500, P=.120), with Bayesian analysis providing
445 anecdotal evidence favoring the null (BF_{10}=0.481).

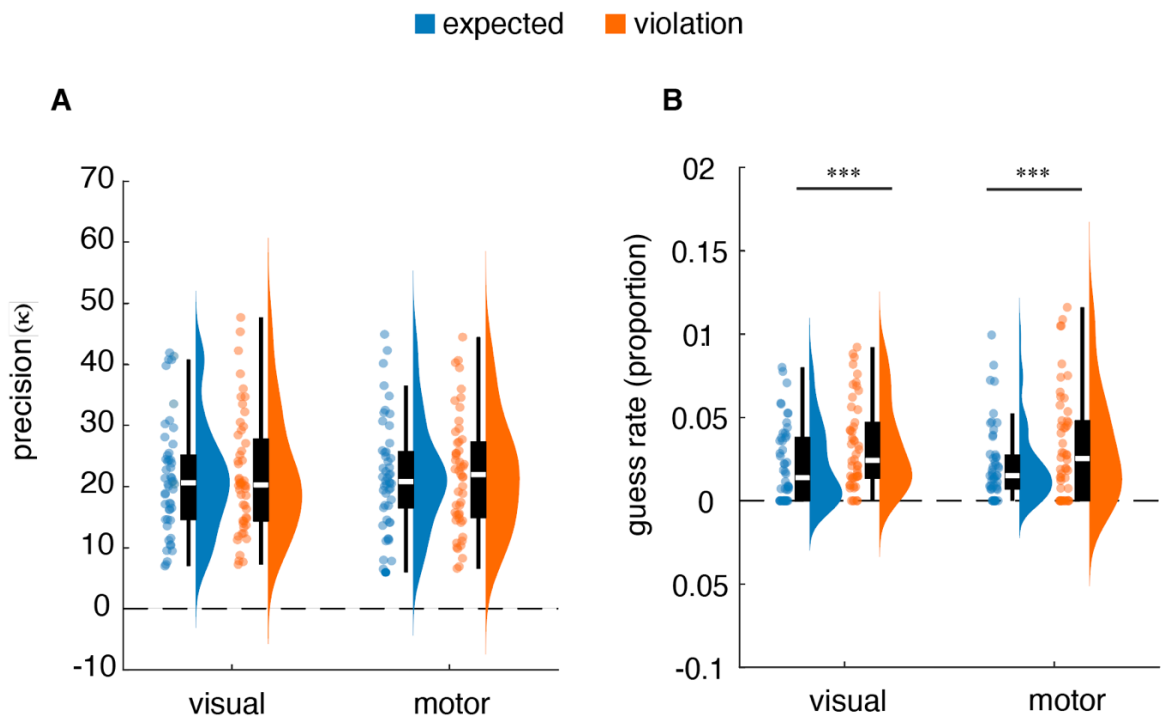

446 **Figure 4. Replication precision (A) and guess rate (B) by sensorimotor domain and expectancy.**
447 These graphs depict the effect of sensorimotor domain and expectancy on participants' (A)
448 replication precision and (B) guess rate (as estimated from mixture modelling). **A**. κ is an indicator of
449 replication precision, which is inversely related to the width of the von Mises function fit to the data
450 during mixture modelling. Higher κ value define narrower distributions, indicating more precise
451 behavioral responses. **B**. Guess rate is defined as the frequency of participants' guesses during the
452 behavioral task, estimated from mixture modelling. Violin plots visualize the distribution of (A)
453 replication precision and (B) guess rate for each condition, with the median indicated by boxplots
454 within each violin and dots indicate individual participant data points. Significant results (p < .001)
455 are denoted with ***.

456 **3.3. Effect of Expectancy on Overall Neural Activity**

Univariate analysis over the occipital ROI was conducted to investigate the effect of expectancy on changes in the overall neural activity in this region, separately for visual and motor conditions. As shown in **Figure 5**, in the visual condition, there was no evident expectation suppression effect, such that no significant differences were shown in the response to expected and violation trials. However, in the motor condition, there were several periods in which significant differences were found between expected and violation trials. In particular, there was a difference observed around 250 ms post-stimulus onset, exhibiting significantly greater P300 activity in violation trials than expected trials. This finding aligns with previous literature, which associates heightened P300 activity in parieto-occipital regions (referred to as 'P3b') with the processing of unlikely events (Polich, 2007). However, from -200 ms to 100 ms around the target stimulus onset, neural responses in expected trials were significantly larger than those in violation trials. Given the timing of this difference, it could not be attributed to target stimulus processing.

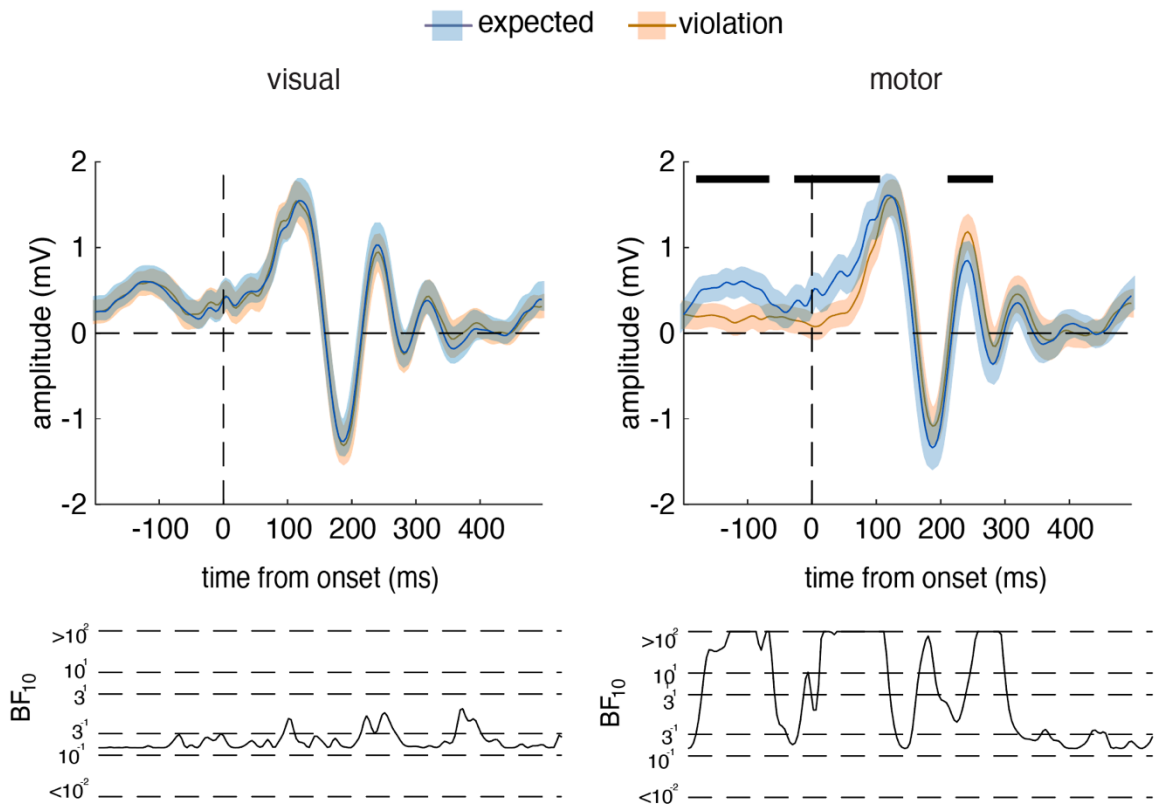

Figure 5. Effect of expectancy on univariate EEG results in visual and motor conditions. These graphs depict the effect of expectancy on univariate EEG results when epoched to target stimulus onset. Shaded areas indicate $\pm$ 1 standard error. Cluster corrected time periods of significant differences between expected and violation trials ($p < 0.05$) are marked with black bars at the top. The bottom sub-panels show the corresponding Bayes Factors (BF_{10}).

The univariate differences in the first half of the epoch of the motor condition may be attributed to pre-stimulus baseline differences due to the temporal delay in target-stimulus onset introduced during motor violation trials. This pre-stimulus onset difference thus motivated us to conduct a *post hoc* analysis of neural activity epoched to 200 ms before and 500 ms after the onset of motor cue for the motor condition (**Figure 6**). We found that the univariate neural response significantly differed after the motor-cue onset, specifically, a greater response was observed in the expected trials from ~50 ms to ~200 ms following the motor cue onset.

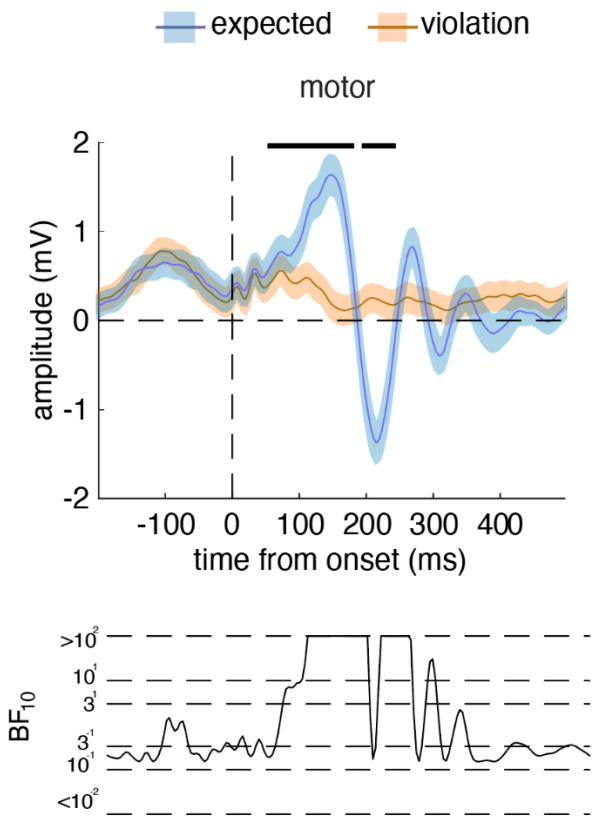

Figure 6. Univariate EEG results in the motor condition epoched to motor-cue onset. This graph depicts the effect of expectancy on univariate EEG results in the motor condition when epoched to motor cue onset (0 in x-axis indicates when motor cues appeared). Shaded areas indicate ± 1 standard error. Cluster corrected time periods of significant differences between expected and violation trials ($p < 0.05$) are marked black bars at the top. The bottom sub-panel shows the corresponding Bayes Factors (BF_{10}).

3.4. Effect of Expectancy on Neural Representation

3.4.1 Feature Decoding: Inverted encoding Modelling

We found some evidence for a univariate expectancy effect in the motor condition, but none in the visual condition; however, univariate analyses can obscure

meaningful multivariate changes in neural activity (Buhmann et al., 2024). Thus, to further explore whether expectancy influenced the neural representation of stimuli we employed inverted encoding to decode feature-selective neural representations, where higher decoding accuracy indicates more precise neural representation of the stimulus. As depicted in **Figure 7**, no significant differences in decoding accuracy were found between expected and violation trials in either the visual or motor conditions. The Bayes factors similarly provided anecdotal evidence for the null hypothesis, supporting the absence of an expectancy effect on stimulus representations.

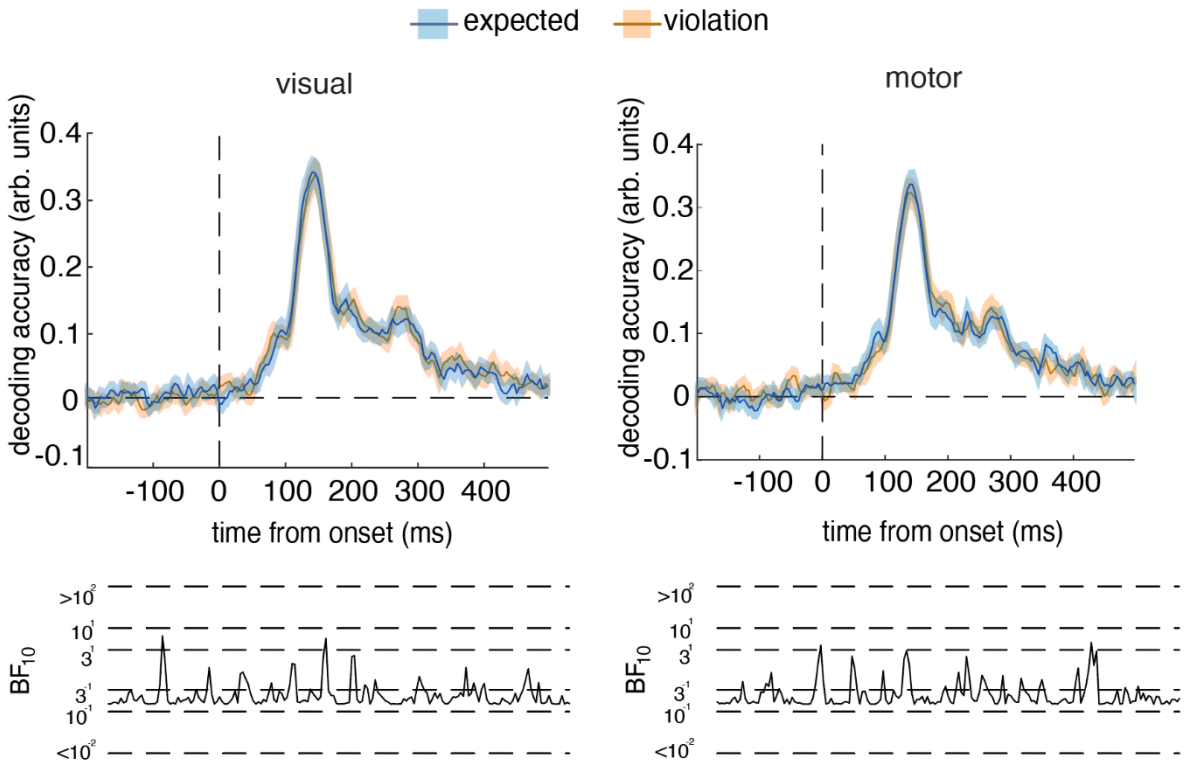

Figure 7. Effect of expectancy on feature decoding in visual and motor conditions. The graphs depict the decoding accuracy for the target stimulus orientation in expected (blue) and violation (orange) trials, for visual and motion conditions (0 in x-axis indicates when the target stimulus appeared), as a function of time. Shaded areas indicate ± 1 standard error. The bottom sub-panels plot the corresponding Bayes Factors (BF_{10}).

3.4.2 Expectancy Decoding: Post-Hoc Linear Discriminant Analysis

In our *a priori* analysis, we intended to examine the correlation between participants' behavioral precision and feature-selective neural precision for target stimuli as the function of expectancy. However, as no significant effects of expectancy were found in either behavioral or stimulus-selective neural precision, this analysis was not conducted. Instead, we performed a *post hoc* linear discriminant

analysis on the EEG data to explore whether trial expectancy, rather than feature-specific representational fidelity, was encoded in the neural activity. That is, we tested whether there were stimulus non-specific differences in the multivariate pattern of activity between expected and violation trials, separately for visual and motor conditions.

As shown in the **Figure 8**, classification accuracy of trial expectancy in the visual condition was not significantly different from the chance level (50% accuracy), except at a brief late period (~350 – 400 ms after target-stimulus onset). The Bayes factor provides similar anecdotal evidence supporting the null hypothesis. In contrast, classification accuracy for the motor condition was consistently significantly above chance level for the entire epoch.

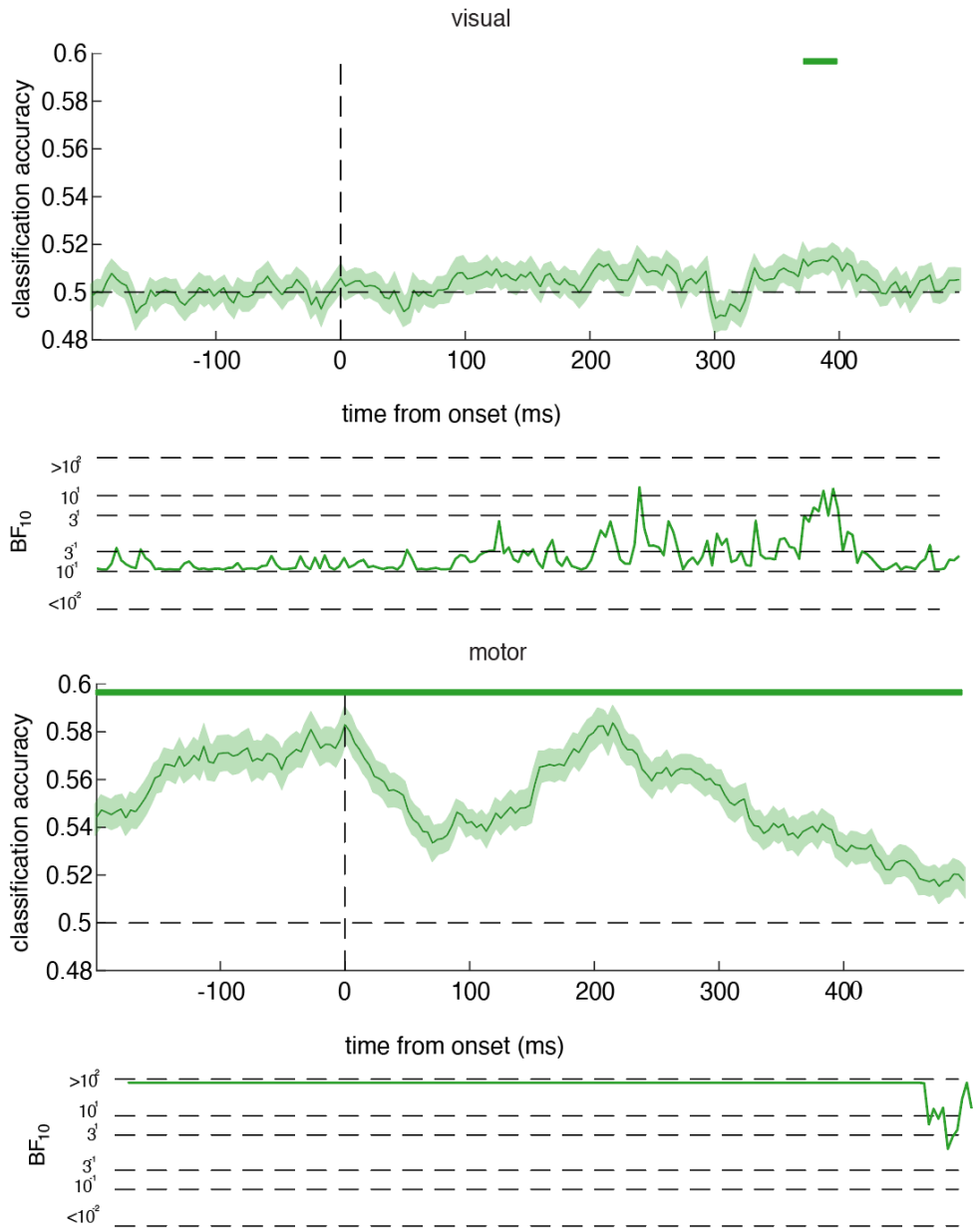

Figure 8. Classification accuracy of trial expectancy in visual and motor conditions. These graphs depict the trial expectancy classification accuracy in (A) visual and (B) motor conditions, epoched to the target-stimulus onset (0 in x-axis indicates when target stimulus appeared). Shaded areas indicate ± 1 standard error. Cluster corrected time periods of significant differences between classification accuracy and chance-level ($p < 0.05$) are marked green bars at the top. The bottom sub-panel shows the corresponding Bayes Factors (BF_{10}).

The LDA results in the motor condition mirrored the significant pre-stimulus differences observed in the univariate EEG analysis. To further investigate the nature of these pre-stimulus differences, we re-epoched the EEG recordings to between 200 ms before and 500 ms after motor cue onset, aligning with the previous *post hoc* analysis. As illustrated in **Figure 9**, classification accuracy for the motor condition was significantly above chance level, starting from ~100 ms post motor-cue onset.

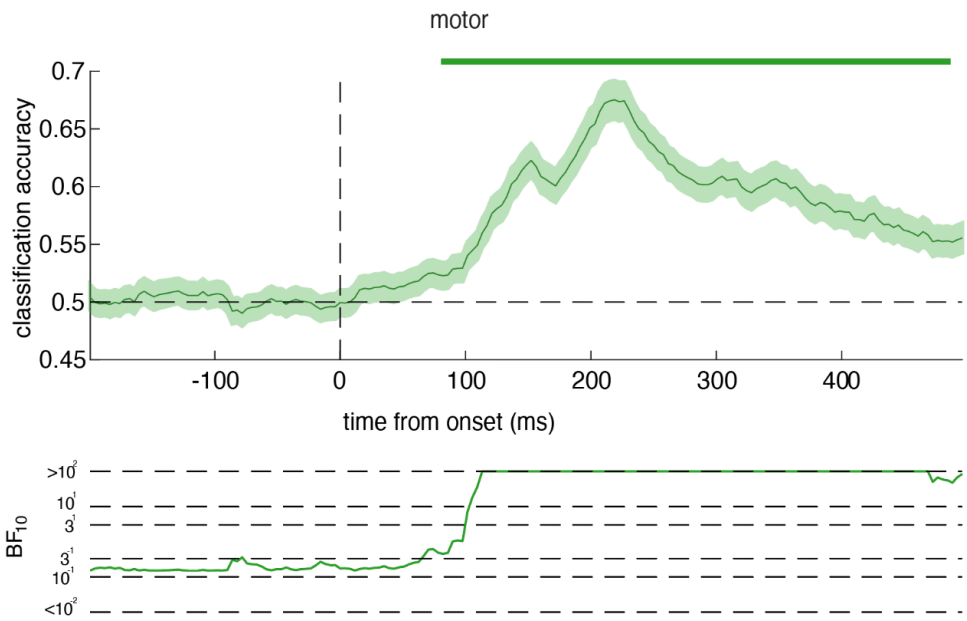

Figure 9. Classification accuracy of trial expectancy in the motor condition epoched to motor-cue onset. The graph depicts the trial expectancy classification accuracy in the motor condition, epoched to the motor-cue onset (0 in x-axis indicates when motor cues appeared). Shaded areas indicate ± 1 standard error. Cluster corrected time periods of significant differences between classification accuracy and chance-level ($p < 0.05$) are marked with green bars at the top. The bottom sub-panel shows the corresponding Bayes Factors (BF_{10}).

3.5. Effect of Expectancy on Pupil Response

In addition to neural and behavioural recordings**,** pupil diameter was recorded to cross-validate whether expectancy was successfully manipulated in our experimental design. We epoched the pupillometry recordings to between 500 ms before and 1500 after target-stimulus onset. Given that both univariate and linear discriminant analyses of EEG recordings revealed pre-stimulus differences, baseline correction was not applied to the pupillometry data, as this would introduce spurious post-stimulus differences. Based on **Figure 10**, no significant difference in pupil diameter was observed between expected and violation trials in the visual condition. The Bayes factor provides substantial evidence in support of the null hypothesis. However, pupil diameter was significantly larger for expected trials than violation trials in the motor condition at 500 ms before stimulus onset, with the Bayes factor suggesting similar decisive evidence for the alternative hypothesis. This pattern was inverted, such that larger pupil diameter was found in violation trials than expected trials ~600 ms after stimulus onset and persisted to ~1300 ms post-stimulus onset.

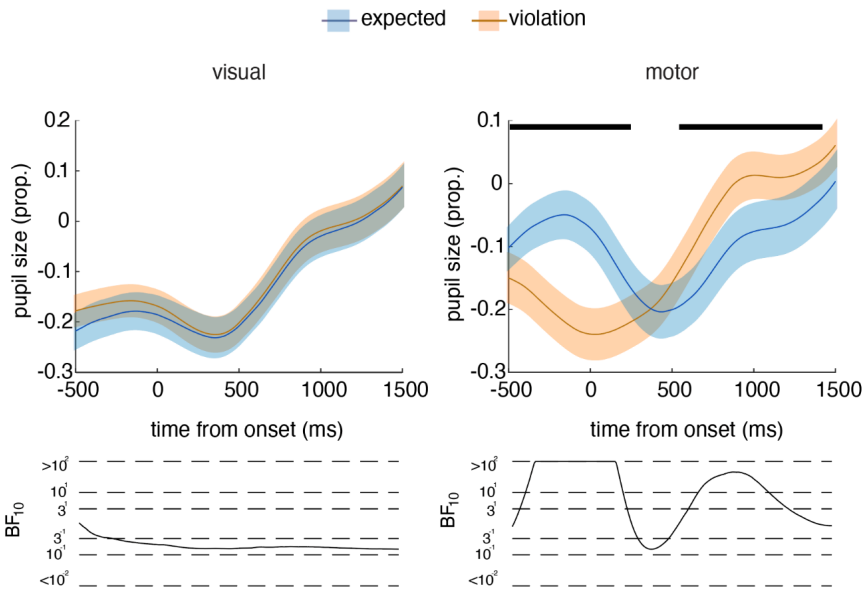

Figure 10. Effect of expectancy on pupil diameter in visual and motor conditions. These graphs show participants' proportional pupil diameter in the expected (blue) and violation (orange) trials, as a function of time from target stimulus onset, separately for visual and motor conditions (0 in x-axis marks the onset of target stimulus). Shaded areas indicate ± 1 standard error. Cluster corrected time periods of significant differences between expected and violation trials ($p < 0.05$) are marked with black bars at the top. The bottom sub-panels show the corresponding Bayes Factors (BF_{10}).

4. DISCUSSION

In this study, we aimed to test whether expectation suppression arises from the sharpening or dampening of neurons selective to expected features, and how predictions interact across sensorimotor domains. Using a novel cross-domain probabilistic cueing paradigm, we combined EEG-based inverted encoding, a continuous reproduction task, and pupillometry, to assess neural, behavioral, and physiological responses to visual and motor expectancies. Our results suggest that while a general expectancy effect was consistently present across multiple measures in the motor condition, this effect did not appear to modulate feature-specific sensory representations, which might be indicative of a hierarchical organization of predictive processing. In contrast, the inconsistent visual expectancy effects align with prior studies reporting challenges in establishing stable neural predictions for visual stimuli using probabilistic cueing paradigms (den Ouden et al., 2023; den Ouden et al., 2024). Given the lack of clear expectancy effects in both domains, the secondary aim of assessing cross-domain integration was not pursued. The implications of these findings for predictive processing and future experimental designs are discussed later.

4.1. No Evidence for Expectancy-Driven Modulation on Sensory Representations

4.1.1 Evaluating Expectation Suppression

Predictive coding theories propose that expectation suppression reflects reduced neural activity for expected stimuli, driven by decreased prediction-error signaling (Friston, 2005; Walsh et al., 2020). However, in the visual condition, our univariate analyses did not reveal significant reductions in general neural activity for expected compared to violation trials. This suggests either insufficient prediction error generation or a failure to establish neural predictions (den Ouden et al., 2023). Given that target stimuli in violation condition were perceptually distinct (>30° difference in orientation), the absence of expectancy effects likely supports the latter explanation – that neural predictions were not sufficiently formed. Similar findings have been reported in electrophysiological studies examining probabilistic cueing paradigms for both high-level (e.g., faces, den Ouden et al., 2023) and low-level (Gabor gratings, den Ouden et al., 2024) visual stimuli.

While the visual condition showed no strong evidence of expectancy suppression, the motor condition exhibited a potential P300 suppression effect around 250 ms post-stimulus onset (Polich, 2007; Saurels et al., 2022). However, earlier neural activity (from 200 ms before to 100 ms after stimulus onset) showed the opposite trend. This reversal suggests that a pre-stimulus baseline difference may have influenced the later suppression effect. The pre-stimulus difference is likely due to the task's temporal structure; inherent in our manipulation of motor expectancy is a delay to the onset of the target stimulus. In expected trials, the immediate onset of the target stimulus after button release likely carried residual motor and visual neural activity, whereas the delay in violation trials may have allowed this activity to stabilize. Regardless of the reason, the pre-stimulus difference makes interpretation of the post-stimulus difference difficult. Supporting this, a post-hoc univariate analysis re-epoched to the motor cue onset revealed larger neural responses in motor expected trials around 100 ms post-cue onset.

4.1.2 Evaluating Neural Representational Fidelity

An alternative interpretation of the opposing pre- and post-stimulus trends is that the later P300 suppression may reflect a genuine expectancy-driven suppression superimposed upon a rebound artifact. However, univariate analyses may fail to capture subtle representational differences that could better explain these effects. Multivariate approaches offer a more sensitive method for examining how expectancy modulates sensory representations (Buhmann et al., 2024). However, our inverted encoding results revealed no significant differences in fidelity between expected and violation conditions, suggesting that both types of events were encoded with similar precision in the current study, supporting neither sharpening nor dampening accounts. These findings appear to contradict hierarchical predictive coding models, which propose that prediction errors should modulate sensory representations (Friston, 2005; Kok & de Lange, 2015). Given the noticeable behavioural difference in response to expected and violation stimuli, the lack of decoding differences suggests that expectancy manipulations in the current study might not be effectively translated into neural predictions. One alternative theory on predictive processing, the opponent-processing theory (Press et al., 2020), proposes that the brain initially prioritizes expected stimuli, shifting toward unexpected stimuli only when strong

expectancy violations occur. Thus, the null fidelity difference between expected and violation conditions may reflect a co-existence of both sharpening and dampening of neurons selective to expected features. However, if this were the case, we would expect temporal transitions in decoding accuracy reflecting this shift, which were not observed in our results. Instead, they are more likely explained by failure to elicit stimulus-specific neural expectations in the current experimental paradigm.

4.1.3 Behavioral and Physiological Expectancy Effects

While our inverted encoding modelling results provide no evidence for sharpening or dampening accounts, the behavioral and physiological data revealed general expectancy effects, particularly in the motor condition. Mixture modelling of the reproduction task revealed that expectancy had no effect on perceptual fidelity, aligning with neural analyses. However, violation trials elicited a higher guess rate in both visual and motor conditions, suggesting a general effect of expectancy on response behaviour. Rather than modulating sensory precision, unexpected events may disrupt attentional processes, leading to more frequent non-informative responses (Maunsell & Treue, 2006). This aligns with findings using attentional blink paradigms, where expectancy violations, particularly unexpected temporal delays, compromise task performance by interfering with attentional allocations (Tang et al., 2014).

Physiological data further supports the observed expectancy effects in the motor condition. Pupil dilation responses were significantly larger in motor violation trials, consistent with prior research linking pupil size to surprise-related noradrenergic arousal (Lavín et al., 2013; Preuschoff et al., 2011). This result aligns with the behavioral and univariate neural findings, suggesting a potential general expectancy effect in the motor condition that is not specific to a particular stimulus feature. However, these results must be interpreted with a note of caution. A significant pre-stimulus difference was observed, with larger pupil diameters in expected trials compared to violation trials. Given that pupil size inversely correlates with environmental luminance (Pan et al., 2022), the brightness contrast between the motor cue (bright) and target stimulus (dim) may have contributed to baseline diameter differences, potentially confounding expectancy-related effects. Similarly, the pre-stimulus differences in pupil size may reflect the intended differences in a

state of surprise but is capturing the motor delay period when participants experience temporal violation. In contrast, no significant pupil dilation differences were observed in the visual condition, aligning with the null results found in neural measures. Consistent neural, behavioral, and physiological findings in the motor condition tentatively suggest that motor-based predictions may have elicited a feature-non-specific expectancy signal. In contrast, inconsistent evidence across the visual condition suggests that visual expectancy in the current study may require stronger reinforcement.

4.2. Hierarchical Predictive Mechanisms: Broad vs. Feature-Specific Predictions

One key pattern of the current results was that, across multiple measures, expectancy effects in the motor condition appeared feature-non-specific, as observed in increased guess rates, P300 suppression, and larger pupil dilation responses in violation trials. However, the absence of expectancy effects in in behavioural precision or inverted encoding modelling suggests that these broad predictions did not modulate the fidelity of sensory representations, contradicting both sharpening and dampening accounts (de Lange et al., 2018; Press et al., 2020). This contrast in results could be indicative of a hierarchical organization of predictive processing, in which broad expectancy effects observed in the motor condition may emerge at a general level but do not necessarily translate into feature-specific neural predictions. This distinction is critical in understanding how expectancy effects could manifest at different levels of neural processing (Munn et al., 2024; Plikat et al., 2025). We further examined this via *post hoc* LDA, which revealed consistently above-chance classification accuracy for trial expectancy in the motor condition, whereas the visual condition showed only a weak, late-stage expectancy-related effect. Notably, pre-stimulus differences in the motor condition mirrored univariate findings. To investigate this, we similarly re-epoched the motor LDA to the motor-cue onset, which exhibited significant above-chance classification accuracy at approximately 100 ms post-cue onset. Since LDA only captures differences between classes of data (Subasi, 2020), there are two possible interpretations for this post-cue result: on one hand, the difference could be driven by visual-field disparities between expected (seeing the target stimulus) and violation (not seeing until after a delay) trials; on the

other hand, the difference might genuinely arise from the expectancy violation caused by the delay in violation trials (i.e., experiencing a delay when something is expected to occur immediately). These results reinforce the idea that expectancy effects in the motor condition were possibly feature-non-specific, and the lack of robust LDA decoding in the visual condition further supports the interpretation that visual expectancy, in the current experimental paradigm, might require stronger reinforcement to manifest.

4.3. Motor-Visual Discrepancy: Context-Independent vs. Context-Dependent Predictions

The persistently observed motor-visual discrepancy in our results diverges from existing predictive coding theories and research (Kok et al., 2014; Rao & Ballard, 1999; Tang et al., 2018), which predominantly focus on the predictive processing in the visual system. One possible explanation is that such discrepancy reflects a fundamental distinction between context-independent and context-dependent forms of predictions (Teufel & Fletcher, 2020). Motor expectancy in the current study were based on temporal associations between an action (button press) and the appearance of a target stimulus. This form of prediction could be seen as context-independent, as such temporal regularities are stable across the daily environments and do not require explicit learning. The potential general expectancy effects in the motor condition may therefore reflect the brain's intrinsic sensitivity to regular temporal associations rather than specific predictions formed in the current paradigm. Visual expectancy in this study, however, relied on cue-target associations across a continuous feature space (orientation). This form of prediction is context-dependent, requiring explicit reinforcement through repeated exposure to form strong associations, especially for this study. Supporting this, prior research has successfully induced context-dependent expectancy effects either using simpler, discrete cue-target mappings (e.g., two cue-target associations in Kok et al., 2012), or substantially larger trial numbers (e.g., 5400 trials in Tang et al., 2018). Thus, the lack of visual expectancy effects in this study may reflect insufficient exposure to establish robust context-dependent predictions. Future research could explore whether prolonged training, or restricted cue-target mappings, will assist a stronger establishment of context-dependent predictions.

4.4. Conclusion

While no evidence was found for expectancy-driven modulations on sensory representations, general motor expectancy effects were observed across neural, behavioural, and physiological measures, suggesting that predictive processing may operate hierarchically, with broad expectancy effects existing without modulating feature-specific sensory representations. However, our findings do not resolve the sharpening vs. dampening debate or provide conclusive insights into cross-domain predictions, as expectancy effects were not sufficiently established in the visual condition. Despite this, the consistent motor expectancy effects across multiple measures highlight an intriguing dissociation between context-independent motor predictions and context-dependent visual predictions (Teufel & Fletcher, 2020), in the current study. These results highlighted the need for refined experimental paradigms for future studies – either to more robustly establish context-dependent predictions or to strategically leverage context-independent ones. Collectively, while this study does not fully resolve the theoretical debate, it provides novel insights into the hierarchical organization of predictive processing in addition to the existing literature (Plikat et al., 2025), as well as how to optimize expectation manipulations in the future research.

REFERENCES

Alais, D., & Burr, D. (2004). The ventriloquist effect results from near-optimal bimodal integration. *Current Biology: CB*, *14*(3), 257–262. https://doi.org/10.1016/j.cub.2004.01.029

Bays, P. M., & Husain, M. (2008). Dynamic shifts of limited working memory resources in human vision. *Science (New York, N.Y.)*, *321*(5890), 851–854. https://doi.org/10.1126/science.1158023

Bode, S., Feuerriegel, D., Bennett, D., & Alday, P. M. (2019). The Decision Decoding ToolBOX (DDTBOX)—A Multivariate Pattern Analysis Toolbox for Event-Related Potentials. *Neuroinformatics*, *17*(1), 27–42. https://doi.org/10.1007/s12021-018-9375-z

Brouwer, G. J., & Heeger, D. J. (2011). Cross-orientation suppression in human visual cortex. *Journal of Neurophysiology*, *106*(5), 2108–2119. https://doi.org/10.1152/jn.00540.2011

Buhmann, Z., Robinson, A. K., Mattingley, J. B., & Rideaux, R. (2024). Inverted encoding of neural responses to audiovisual stimuli reveals super-additive multisensory enhancement. *eLife*, *13*. https://doi.org/10.7554/eLife.97230.1

de Lange, F. P., Heilbron, M., & Kok, P. (2018). How Do Expectations Shape Perception? *Trends in Cognitive Sciences*, *22*(9), 764–779. https://doi.org/10.1016/j.tics.2018.06.002

Delorme, A., & Makeig, S. (2004). EEGLAB: An open source toolbox for analysis of single-trial EEG dynamics including independent component analysis. *Journal of Neuroscience Methods*, *134*(1), 9–21. https://doi.org/10.1016/j.jneumeth.2003.10.009

den Ouden, C., Zhou, A., Mepani, V., Kovács, G., Vogels, R., & Feuerriegel, D. (2023). Stimulus expectations do not modulate visual event-related potentials in probabilistic cueing designs. *NeuroImage*, *280*, 120347. https://doi.org/10.1016/j.neuroimage.2023.120347

Den Ouden, H., Friston, K., Daw, N., McIntosh, A., & Stephan, K. (2008). A Dual Role for Prediction Error in Associative Learning. *Cerebral Cortex (New York, N.Y.: 1991)*, *19*, 1175–1185. https://doi.org/10.1093/cercor/bhn161

Friston, K. (2005). A theory of cortical responses. *Philosophical Transactions of the Royal Society B: Biological Sciences*, *360*(1456), 815–836. https://doi.org/10.1098/rstb.2005.1622

Friston, K. (2010). The free-energy principle: A unified brain theory? *Nature Reviews Neuroscience*, *11*(2), 127–138. https://doi.org/10.1038/nrn2787

Gessell, B., Geib, B., & De Brigard, F. (2021). Multivariate pattern analysis and the search for neural representations. *Synthese*, *199*(5–6), 12869–12889. https://doi.org/10.1007/s11229-021-03358-3

Groppe, D. M., Urbach, T. P., & Kutas, M. (2011). Mass univariate analysis of event-related brain potentials/fields I: A critical tutorial review. *Psychophysiology*, *48*(12), 1711–1725. https://doi.org/10.1111/j.1469-8986.2011.01273.x

Hall, M. G., Mattingley, J. B., & Dux, P. E. (2018). Electrophysiological correlates of incidentally learned expectations in human vision. *Journal of Neurophysiology*, *119*(4), 1461–1470. https://doi.org/10.1152/jn.00733.2017

Harrison, W. J., Bays, P. M., & Rideaux, R. (2023). Neural tuning instantiates prior expectations in the human visual system. *Nature Communications*, *14*(1), 5320. https://doi.org/10.1038/s41467-023-41027-w

Jeffreys, H. (1998). *Theory of Probability*. Clarendon Press.

Kok, P., & de Lange, F. P. (2015). Predictive coding in sensory cortex. In *An introduction to model-based cognitive neuroscience* (pp. 221–244). Springer Science + Business Media. https://doi.org/10.1007/978-1-4939-2236-9

Kok, P., Failing, F. M., & de Lange, F. P. (2014). Prior Expectations Evoke Stimulus Templates in the Primary Visual Cortex. *Journal of Cognitive Neuroscience*, *26*(7), 1555–1571. https://doi.org/10.1162/jocn_a_00562

Kok, P., Jehee, J. F. M., & de Lange, F. P. (2012). Less Is More: Expectation Sharpens Representations in the Primary Visual Cortex. *Neuron*, *75*(2), 265–270. https://doi.org/10.1016/j.neuron.2012.04.034

Kok, P., Mostert, P., & de Lange, F. P. (2017). Prior expectations induce prestimulus sensory templates. *Proceedings of the National Academy of Sciences*, *114*(39), 10473–10478. https://doi.org/10.1073/pnas.1705652114

Kuffler, S. W. (1953). Discharge patterns and functional organization of mammalian retina. *Journal of Neurophysiology*, *16*(1), 37–68. https://doi.org/10.1152/jn.1953.16.1.37

Lavín, C., San Martín, R., & Rosales Jubal, E. (2013). Pupil dilation signals uncertainty and surprise in a learning gambling task. *Frontiers in Behavioral Neuroscience*, *7*, 218. https://doi.org/10.3389/fnbeh.2013.00218

Lee, K., & Rideaux, R. (2024). *The influence of temporal context on vision over multiple time scales* (p. 2024.10.27.620542). bioRxiv. https://doi.org/10.1101/2024.10.27.620542

Lotter, W., Kreiman, G., & Cox, D. (2020). A neural network trained for prediction mimics diverse features of biological neurons and perception. *Nature*

Machine Intelligence, *2*(4), 210–219. https://doi.org/10.1038/s42256-020-0170-9

Maris, E., & Oostenveld, R. (2007). Nonparametric statistical testing of EEG- and MEG-data. *Journal of Neuroscience Methods*, *164*(1), 177–190. https://doi.org/10.1016/j.jneumeth.2007.03.024

Maunsell, J. H. R., & Treue, S. (2006). Feature-based attention in visual cortex. *Trends in Neurosciences*, *29*(6), 317–322. https://doi.org/10.1016/j.tins.2006.04.001

Mazancieux, A., Mauconduit, F., Amadon, A., Willem de Gee, J., Donner, T. H., & Meyniel, F. (2023). Brainstem fMRI signaling of surprise across different types of deviant stimuli. *Cell Reports*, *42*(11), 113405. https://doi.org/10.1016/j.celrep.2023.113405

Mostert, P., Kok, P., & de Lange, F. P. (2015). Dissociating sensory from decision processes in human perceptual decision making. *Scientific Reports*, *5*(1), 18253. https://doi.org/10.1038/srep18253

Munn, B. R., Müller, E. J., Favre-Bulle, I., Scott, E., Lizier, J. T., Breakspear, M., & Shine, J. M. (2024). Multiscale organization of neuronal activity unifies scale-dependent theories of brain function. *Cell*, S0092867424011528. https://doi.org/10.1016/j.cell.2024.10.004

Oostenveld, R., & Praamstra, P. (2001). The five percent electrode system for high-resolution EEG and ERP measurements. *Clinical Neurophysiology: Official Journal of the International Federation of Clinical Neurophysiology*, *112*(4), 713–719. https://doi.org/10.1016/s1388-2457(00)00527-7

Ouden, C. den, Kashyap, M., Kikkawa, M., & Feuerriegel, D. (2024). *Limited evidence for probabilistic cueing effects on grating-evoked event-related potentials and orientation decoding performance* (p. 2024.05.26.595980). bioRxiv. https://doi.org/10.1101/2024.05.26.595980

Pan, J., Klímová, M., McGuire, J. T., & Ling, S. (2022). Arousal-based pupil modulation is dictated by luminance. *Scientific Reports*, *12*(1), 1390. https://doi.org/10.1038/s41598-022-05280-1

Pelli, D. G. (1997). *The VideoToolbox software for visual psychophysics: Transforming numbers into movies*. https://doi.org/10.1163/156856897X00366

Plikat, V., Grassi, P. R., Frack, J., & Bartels, A. (2025). Hierarchical surprise signals in naturalistic violation of expectations. *Imaging Neuroscience*, *3*, imag_a_00459. https://doi.org/10.1162/imag_a_00459

Polich, J. (2007). Updating P300: An Integrative Theory of P3a and P3b. *Clinical Neurophysiology : Official Journal of the International Federation of Clinical Neurophysiology*, *118*(10), 2128–2148. https://doi.org/10.1016/j.clinph.2007.04.019

Press, C., Kok, P., & Yon, D. (2020). The Perceptual Prediction Paradox. *Trends in Cognitive Sciences*, *24*(1), 13–24. https://doi.org/10.1016/j.tics.2019.11.003

Preuschoff, K., ’t Hart, B. M., & Einhauser, W. (2011). Pupil Dilation Signals Surprise: Evidence for Noradrenaline’s Role in Decision Making. *Frontiers in Neuroscience*, *5*. https://doi.org/10.3389/fnins.2011.00115

Rao, R. P. N., & Ballard, D. H. (1999). Predictive coding in the visual cortex: A functional interpretation of some extra-classical receptive-field effects. *Nature Neuroscience*, *2*(1), 79–87. https://doi.org/10.1038/4580

Rideaux, R. (2024). Task-related modulation of event-related potentials does not reflect changes to sensory representations. *Imaging Neuroscience*, *2*, 1–13. https://doi.org/10.1162/imag_a_00266

Rideaux, R., Dang, P., Jackel-David, L., Buhmann, Z., Rangelov, D., & Mattingley, J. B. (2024). *Violated predictions enhance the representational fidelity of visual features in perception*. https://doi.org/10.1101/2024.03.27.587109

Rideaux, R., Storrs, K. R., Maiello, G., & Welchman, A. E. (2021). How multisensory neurons solve causal inference. *Proceedings of the National Academy of Sciences*, *118*(32), e2106235118. https://doi.org/10.1073/pnas.2106235118

Rideaux, R., & Welchman, A. E. (2018). Proscription supports robust perceptual integration by suppression in human visual cortex. *Nature Communications*, *9*(1), 1502. https://doi.org/10.1038/s41467-018-03400-y

Rideaux, R., West, R. K., Rangelov, D., & Mattingley, J. B. (2023). Distinct early and late neural mechanisms regulate feature-specific sensory adaptation in the human visual system. *Proceedings of the National Academy of Sciences*, *120*(6), e2216192120. https://doi.org/10.1073/pnas.2216192120

Roe, A. W., Chelazzi, L., Connor, C. E., Conway, B. R., Fujita, I., Gallant, J. L., Lu, H., & Vanduffel, W. (2012). Toward a unified theory of visual area V4. *Neuron*, *74*(1), 12–29. https://doi.org/10.1016/j.neuron.2012.03.011

Saurels, B. W., Arnold, D. H., Anderson, N. L., Lipp, O. V., & Yarrow, K. (2022). The perceived duration of expected events depends on how the expectation is

formed. *Attention, Perception & Psychophysics*, *84*(5), 1718–1725. https://doi.org/10.3758/s13414-022-02519-x

Smout, C. A., Tang, M. F., Garrido, M. I., & Mattingley, J. B. (2019). Attention promotes the neural encoding of prediction errors. *PLoS Biology*, *17*(2), e2006812. https://doi.org/10.1371/journal.pbio.2006812

Stanford, T. R., Quessy, S., & Stein, B. E. (2005). Evaluating the Operations Underlying Multisensory Integration in the Cat Superior Colliculus. *Journal of Neuroscience*, *25*(28), 6499–6508. https://doi.org/10.1523/JNEUROSCI.5095-04.2005

Stein, B. E., & Stanford, T. R. (2008). Multisensory integration: Current issues from the perspective of the single neuron. *Nature Reviews Neuroscience*, *9*(4), 255–266. https://doi.org/10.1038/nrn2331

Stekelenburg, J. J., & Vroomen, J. (2015). Predictive coding of visual–auditory and motor-auditory events: An electrophysiological study. *Brain Research*, *1626*, 88–96. https://doi.org/10.1016/j.brainres.2015.01.036

Subasi, A. (2020). *Practical Machine Learning for Data Analysis Using Python*.

Summerfield, C., Wyart, V., Johnen, V. M., & de Gardelle, V. (2011). Human Scalp Electroencephalography Reveals that Repetition Suppression Varies with Expectation. *Frontiers in Human Neuroscience*, *5*, 67. https://doi.org/10.3389/fnhum.2011.00067

Sun, J., & Perona, P. (1998). Where is the sun? *Nature Neuroscience*, *1*(3), 183–184. https://doi.org/10.1038/630

Tang, M. F., Badcock, D. R., & Visser, T. A. W. (2014). Training and the attentional blink: Limits overcome or expectations raised? *Psychonomic Bulletin & Review*, *21*(2), 406–411. https://doi.org/10.3758/s13423-013-0491-3

Tang, M. F., Kheradpezhouh, E., Lee, C. C. Y., Dickinson, J. E., Mattingley, J. B., & Arabzadeh, E. (2023). Expectation violations enhance neuronal encoding of sensory information in mouse primary visual cortex. *Nature Communications*, *14*(1), 1196. https://doi.org/10.1038/s41467-023-36608-8

Tang, M. F., Smout, C. A., Arabzadeh, E., & Mattingley, J. B. (2018). Prediction error and repetition suppression have distinct effects on neural representations of visual information. *eLife*, *7*, e33123. https://doi.org/10.7554/eLife.33123

Teufel, C., Dakin, S. C., & Fletcher, P. C. (2018). Prior object-knowledge sharpens properties of early visual feature-detectors. *Scientific Reports*, *8*(1), 10853. https://doi.org/10.1038/s41598-018-28845-5

Teufel, C., & Fletcher, P. C. (2020). Forms of prediction in the nervous system. *Nature Reviews. Neuroscience*, *21*(4), 231–242. https://doi.org/10.1038/s41583-020-0275-5

Todorovic, A., van Ede, F., Maris, E., & de Lange, F. P. (2011). Prior Expectation Mediates Neural Adaptation to Repeated Sounds in the Auditory Cortex: An MEG Study. *The Journal of Neuroscience*, *31*(25), 9118–9123. https://doi.org/10.1523/JNEUROSCI.1425-11.2011

Tran, D. M. D., & Livesey, E. J. (2021). Prediction-based attenuation as a general property of learning in neural circuits. *Journal of Experimental Psychology. Animal Learning and Cognition*, *47*(1), 14–24. https://doi.org/10.1037/xan0000280

Tran, D. M. D., McNair, N. A., Harris, J. A., & Livesey, E. J. (2021). Expected TMS excites the motor system less effectively than unexpected stimulation. *NeuroImage*, *226*, 117541. https://doi.org/10.1016/j.neuroimage.2020.117541

Tran, D. M. D., McNair, N. A., Whitton, A. E., Whitford, T. J., & Livesey, E. J. (2025). *Sensory prediction errors predict motor prediction errors* (p. 2025.03.16.643175). bioRxiv. https://doi.org/10.1101/2025.03.16.643175

Walsh, K. S., McGovern, D. P., Clark, A., & O'Connell, R. G. (2020). Evaluating the neurophysiological evidence for predictive processing as a model of perception. *Annals of the New York Academy of Sciences*, *1464*(1), 242–268. https://doi.org/10.1111/nyas.14321

Zhang, W., & Luck, S. J. (2008). Discrete fixed-resolution representations in visual working memory. *Nature*, *453*(7192), 233–235. https://doi.org/10.1038/nature06860